Contact network in nearly jammed disordered packings of hard-sphere chains

Nikos Ch. Karayiannis, Katerina Foteinopoulou, and Manuel Laso*
Institute for Optoelectronics and Microsystems (ISOM) and ETSII, Universidad Politécnica de Madrid (UPM), José Gutiérrez Abascal 2, E-28006 Madrid, Spain
(Received 27 April 2009; published 20 July 2009)

We present salient results of the analysis of the geometrical structure of a large fully equilibrated ensemble of nearly jammed packings of linear freely jointed chains of tangent hard spheres generated via extensive Monte Carlo simulations. In spite the expected differences due to chain connectivity, both the pair-correlation function and the contact network for chain packings are found to strongly resemble those in packings of monomeric hard spheres at the maximally random jammed (MRJ) state. A remarkable finding of the present work is the tendency of chains to form closed loops at the MRJ state as a consequence of chain collapse. Our simulations on disordered nearly jammed chain packings yield an average coordination number of 6, which fulfills the isostaticity condition and is in excellent agreement with the corresponding simulation [A. Donev, S. Torquato, and F. H. Stillinger, Phys. Rev. E **71**, 011105 (2005)] and experimental [T. Aste, M. Saadatfar, and T. J. Senden, Phys. Rev. E **71**, 061302 (2005)] findings for jammed packings of monatomic hard spheres. An exact correspondence between the statistical-mechanical ensembles of monomeric spheres and of hard-sphere chains offers insights regarding the structure and topology of the contact network of hard-sphere systems at the MRJ state.

DOI: 10.1103/PhysRevE.80.011307 PACS number(s): 45.70.−n, 61.20.−p, 05.20.−y

I. INTRODUCTION

In the last years structural properties and topological characteristics of amorphous jammed [1] or nearly jammed ensamples of hard spheres and other hard-body objects have been the subject of extensive experimental, theoretical, and modeling research [2–15], following the classical studies by Bernal and co-workers [16–18] on dense random packings. Furthermore, by introducing the concept of the maximally random jammed state (MRJ), Torquato *et al.* [1] established the basis for a more rigorous statistical-mechanical description of the random close packing than previously available [18]. The increased scientific interest for model ordered or random assemblies of hard-core species is not surprising given the significant impact in a wide range of processes and applications of physical systems from colloids, emulsions, and granular materials to mathematics and communication theory [19–23].

Compared to monatomic analogs, random packings of freely jointed chains of tangent hard spheres present significant difficulties in their simulation-based studies arising primarily from the intramolecular holonomic constraints (chain connectivity) and from the long relaxation times due to sluggish reptation dynamics [24] owing to intermolecular topological constraints. As a consequence from the modeling perspective, the generation and the successive full-scale equilibration of dense hard-sphere chain systems especially in the vicinity of the MRJ state are by no means trivial. State-of-the-art algorithms [25–27] with well-documented efficiency for the generation of dense or maximally jammed random packings of monomeric hard spheres are not applicable to macromolecular systems because of the imposed chain connectivity. In addition, algorithmic schemes based on the construction of chain assemblies from monatomic-sphere analogs through site-bridging techniques of self-avoiding bonds are unable to properly sample the configurational space, thus leading to incorrect global and local chain conformations and statistical averages of observables. In parallel, the performance of advanced Monte Carlo (MC) techniques that perform exceptionally well in equilibrating atomistic or coarse-grained polymer melts [28] deteriorates as volume fractions of random hard-sphere chain assemblies exceed the freezing transition.

While an appreciable body of modeling studies on hard-sphere chain systems exists at dilute and intermediate volume fractions (packing densities) [29–38] the generation and the efficient sampling of polymer configurations in the close vicinity of the MRJ state require very extensive simulations based on a novel MC suite built around advanced chain-connectivity-altering moves [39]. Through such a MC scheme, we were recently able to determine the MRJ state of hard-sphere chain assemblies [40], to analyze the effect of concentration (packing density) on chain size [41–43], on structure [44], and on the underlying network of topological hindrance [42,43], both as entanglements and knots. Very recently our modeling studies were extended to track the entropy-driven disorder-order transition of dense hard-sphere chain systems [45], the onset, and the growth of crystal nuclei and the spontaneous formation of characteristic crystal morphologies [46].

In the present paper, we present results and analyze the salient features of the contact network of a large ensemble of freely jointed chains of tangent hard spheres in the close vicinity of the MRJ state generated through MC simulations. We show that these jammed chain packings are particularly useful for elucidating structural aspects in the corresponding assemblies of monomeric hard spheres. In the Appendix we discuss the statistical-mechanical basis of the correspondence between jammed packings of *chains* of tangent hard spheres

*Author to whom correspondence should be addressed; mlaso@etsii.upm.es

and packings of *monatomic* spheres at their MRJ. We find that the former can, in a natural way, shed light on key features of the structure of the latter that may, for numerical reasons, remain elusive even to very precise analyses.

II. SIMULATION DETAILS

All reported MC simulations were conducted in the isochoric semigrand canonical ensemble $[VTN_{\text{sites}}\mu^*]$ for two systems of freely jointed linear chains of tangent hard spheres of equal size, both bearing a total of 1200 interacting sites: (1) 100 chains of average length $N=12$ and (2) 50 chains of average length $N=24$ at two different volume fractions: $\varphi=0.63$ and $\varphi^{\text{MRJ}}\simeq 0.639$. Chain lengths were allowed to fluctuate uniformly in the closed intervals $N\in[6,18]$ and $N\in[12,36]$ for the $N=12$ and 24 systems, respectively. Periodic boundary conditions were applied in all dimensions of the cubic cell and simulations were conducted with boxes of varied length to ensure that the chain size, the packing, and the local ordering remain unaffected by the system size. The following mixture of MC moves was employed: simplified end bridging (0.1%), simplified intramolecular end bridging (0.1%), adaptive-bias reptation (10%), adaptive-bias rotation (10%), adaptive configurational bias (20%), adaptive-bias intermolecular reptation (25%), and adaptive-bias flip (34.8%), where numbers in parentheses denote percentage attempt probabilities. The number of trial positions n_{dis} for the forward and the reverse transitions for all moves executed in the adaptive-bias pattern was set equal to $n_{\text{dis}}=70$ at $\varphi=0.63$ and $n_{\text{dis}}=100$ at $\varphi=\varphi^{\text{MRJ}}$. More details about the MC scheme and about its computational efficiency in generating and successively in equilibrating the long- and the short-range chain characteristics as functions of packing density and average chain length can be found in Ref. [39]. Because of the application of the chain-connectivity-altering MC moves, the numerical tolerance for the bond length constraint was set at $\delta\sigma=10^{-8}$ allowing bond lengths to fluctuate in the interval $[\sigma,\sigma+\delta\sigma]$, where σ is the collision diameter of the hard spheres. Compared to our past studies [39–46] the present limit for bond lengths is by four orders of magnitudes stricter. Present data confirm previous findings [47] that the model with fluctuating bond lengths (even with $\delta\sigma\simeq 0.01$) does not present any appreciable differences regarding local packing and chain size with the "pearl and necklace" freely jointed model of strictly tangent hard spheres. Still, recent theoretical predictions suggest that the ratio of bond length to collision diameter affects significantly the ability of model chains to crystallize at high densities [48].

The MC calculations were carried out for 4.0×10^{11} and 2.9×10^{11} MC steps at $\varphi=0.63$ and $\varphi=\varphi^{\text{MRJ}}=0.639$, respectively. Configurations including coordinates of the sphere centers, chain connectivity, and system statistics were recorded every 1×10^7 steps. At $\varphi=0.639$ the fraction of spheres (so called "flippers") that were able to perform a minimal displacement subject to the constraints imposed by chain connectivity and to the overlaps with all fixed spheres in the system is less than 1%, which is a strong indication that the system approaches the maximally random jammed state; at $\varphi=0.63$ the corresponding fraction is much higher as approximately one out of four sites is a flipper [49].

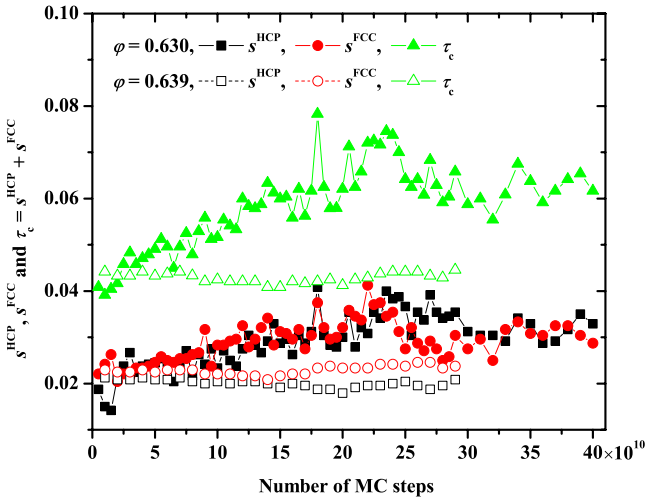

FIG. 1. (Color online) Evolution of the HCP (s^{HCP}) and the FCC (s^{FCC}) order parameters and of their sum ($\tau_c=s^{\text{HCP}}+s^{\text{FCC}}$) as functions of MC steps at packing densities $\varphi=0.63$ (filled symbols) and $\varphi=\varphi^{\text{MRJ}}$ (open symbols). Since the CCE-based order parameters are highly discriminating, the obtained τ_c parameter can be interpreted as an accurate estimate for the total degree of crystallinity.

According to Rintoul and Torquato [50], for long simulation times, packings of monomeric hard spheres tend to crystallize at all packing densities above the melting point. In recent simulations by us, similar conclusions have been drawn for chain assemblies of hard spheres in the concentration interval of $\varphi\in[0.58,0.61]$ [46]. Given the above findings, and since present simulations are exceedingly long [approaching trillion (10^{12}) of MC steps], special care was taken to exclude from the structural analysis those parts of the MC trajectories that could possibly undergo a disorder-order transition, as indicated by the appearance and the rapid growth of crystal nuclei [45], just as it is routinely done in studies of disordered packings of monatomic hard spheres. To this end we analyzed the local structure around each hard-sphere site at specific system configurations (trajectory frames) by means of the characteristic crystallographic element (CCE) norm [40,44–46] that is able to accurately detect any orientational and radial deviations from perfect order and thus track any ordering (or disordering) transitions. Furthermore, the CCE norm is shown to be able to distinguish with high specificity between different competing crystal structures. More technical details about the applicability of the CCE norm on general atomistic and particulate systems can be found in Ref. [45]. In the present work, we proceeded through the Voronoi tessellation (through the qhull program [51]) of the simulation cell and consecutively applied the hexagonal-close-packed (HCP-) and face-centered cubic (FCC-) CCE norms on all sites of the system for selected frames of the MC trajectory every 1×10^9 steps. The information of the HCP-CCE and the FCC-CCE norms was used to calculate the corresponding order parameters s^{HCP} and s^{FCC} [44–46]. Sites with HCP-CCE and FCC-CCE norms below a certain threshold were univocally identified as HCP-like and FCC-like structures, respectively [52]. Figure 1 presents the evolution of the s^{HCP} and the s^{FCC} order parameters along with their sum (τ_c), which can be interpreted as an

estimate for the total degree of crystallinity, as a function of MC steps. It can be seen that in both cases ($\varphi=0.63$ and $\varphi=\varphi^{\mathrm{MRJ}}$) the fractions of sites with either HCP- or FCC-like character change only minimally during the entire MC run. The degree of crystallinity does not exceed 6% and 4% at $\varphi=0.63$ and $\varphi=\varphi^{\mathrm{MRJ}}$, respectively. We should further note that the fluctuations of the individual order parameters and of the total degree of crystallinity are minimal at the MRJ state, as expected in a jammed system. Our observed values for the HCP and the FCC populations of sites are of the same order of magnitude as those found by Aste *et al.* [53] from x-ray computed tomography on samples of monosized spheres. Their analysis based on the rotationally invariant measures of combinations of spherical harmonics [54] suggest HCP and FCC fractions of 8% and 3%, respectively, along with a significant portion of sites with an unidentified local environment [53]. From the data shown in Fig. 1 on the evolution of the individual order parameters and of their sum, it is clear that our MC-generated chain packings remain disordered (random) in all recorded system configurations at both packing densities [55].

III. STRUCTURAL FEATURES OF NEARLY JAMMED RANDOM PACKING OF HARD-SPHERE CHAINS

Donev *et al.* [2] and Aste *et al.* [10] have presented very thorough computational and experimental results, respectively, for the pair radial distribution function $g(r)$ for nearly and maximally jammed disordered packings of single hard spheres. The pair distribution function is a widely used orientationally averaged structural descriptor, and its accurate calculation is of vital importance for the understanding of structural features [10]. Donev *et al.* [2] convincingly showed that, in the jamming limit, $g(r\rightarrow 1^{+})$ separates in a singular, $\delta(r)$, or "contact" contribution, and a "background," or near-contact contribution. Their results also confirmed the isostaticity of MRJ packings and the splitting of the second peak in $g(r)$ as a clear signature of jamming. Recently, beautifully detailed and accurate x-ray tomography results on the three-dimensional structure of large packings of monosized spheres with volume fractions up to the MRJ value have been reported by Aste *et al.* [10] They have derived the radial distribution function and observed a strong peak at a distance equal to the particle diameter σ, followed by a minimum at around 1.4σ and two additional peaks at greater separations $r=\sqrt{3}\sigma$ and $r\approx 2\sigma$ [10]. Their findings confirmed the behavior for $g(r)$ predicted by Donev *et al.* [2] in the region between $r\approx\sigma$ and $r\approx 1.4\sigma$.

Although it seems natural that the ensemble-average properties of MRJ packings of monomeric spheres and of chains must differ due to chain connectivity, it is perhaps not so obvious that they must share several key features as well. The ultimate reason for the similarities is the existence of a correspondence between configurations of monomeric spheres and of hard-sphere chains. As discussed in the Appendix, structural features, for example, peak positions in $g(r)$, although weighted quantitatively differently in the two ensembles, e.g., different peak intensities for $g(r)$ in $\Xi_{\mathrm{ss}}^{\mathrm{MRJ}}$ and $\Xi_{\mathrm{chains}}^{\mathrm{MRJ}}$ (see the Appendix for nomenclature), must necessarily be *geometrically* identical for both systems. For example, the arrangement of spheres and the exact radial position for second peak splitting in $g(r)$ must be the same in both ensembles. A qualitative illustration of the aforementioned correspondence between configurations of monomeric (single) hard spheres and of hard-sphere chains is shown in Fig. 2.

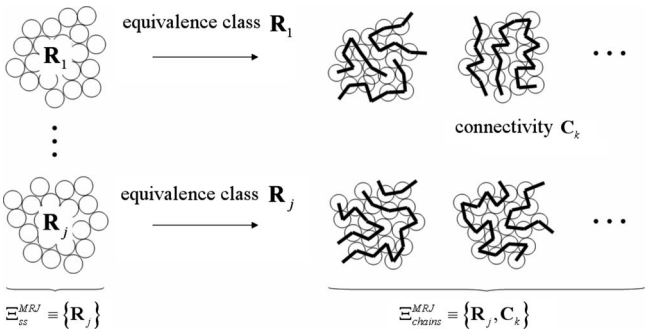

FIG. 2. The ensembles $\Xi_{\mathrm{chains}}^{\mathrm{MRJ}}$ and $\Xi_{\mathrm{ss}}^{\mathrm{MRJ}}$ for hard-sphere chains and single (monatomic) hard spheres, respectively. Each member $(\mathbf{R}_j,\mathbf{C}_k)\in\Xi_{\mathrm{chains}}^{\mathrm{MRJ}}$ is uniquely mappable on a member of $\Xi_{\mathrm{ss}}^{\mathrm{MRJ}}$ by simply deleting chain connectivity. $\Xi_{\mathrm{chains}}^{\mathrm{MRJ}}$ splits naturally in equivalent classes. Each class contains all chain configurations that differ in connectivity $\mathbf{C}_k$ but are mapped on the same $\mathbf{R}_j$.

Combinatorial geometry methods [56] are able to find members of $\Xi_{\mathrm{chains}}^{\mathrm{MRJ}}$ (solutions to the sphere connectivity problem), but these methods do not respect microscopic reversibility, nor do they preserve phase-space volume. The challenge, which was solved by the introduction of the MC protocol of Refs. [39,40], was to generate members of $\Xi_{\mathrm{chains}}^{\mathrm{MRJ}}$ with their correct statistical-mechanical weight. We have to note that even by employing the proposed MC scheme [39–46] much greater computational effort is required to generate chain configurations as compared to monomeric sphere analogs, especially in the close vicinity of the MRJ state. For example, all simulations reported here and above all those for the generation and the relaxation at the highest volume fraction required wall-clock CPU times that reached the order of many months. As a direct consequence, the structures of $\Xi_{\mathrm{chains}}^{\mathrm{MRJ}}$ generated here are jammed (or more precisely nearly jammed) to a less strict numerical tolerance $[O(10^{-4})]$ than those in Ref. [2] where jamming for monatomic hard spheres is detected to almost machine precision $[O(10^{-12})]$. This however does not invalidate the results to be presented, since the correspondence between configurations is equally valid at both tolerance levels. Hence, as argued in the Appendix, the geometric features observed in the chain system are translatable to the MRJ state of monomeric hard spheres. While the related computational cost is significantly increased, we have embarked on simulations of hard-sphere chains at the MRJ state where the precision set for the detection of jamming is comparable with the one in Ref. [2] (i.e., close to machine precision).

In the following we will exploit the relation between $\Xi_{\mathrm{ss}}^{\mathrm{MRJ}}$ and $\Xi_{\mathrm{chains}}^{\mathrm{MRJ}}$ to extract structural information about monomeric (single) hard-sphere packings at the MRJ state. Donev *et al.* [2] recently presented what is probably the most careful in-depth numerical analysis of the characteristics of

the pair-correlation function $g(r)$ of disordered nearly jammed packings of monatomic hard spheres. They were able to generate maximally jammed random packings of hard spheres by event-driven molecular dynamics [57] (a modification of the Lubachevsky-Stillinger algorithm [27,58]). The jammed character of these packings was subsequently tested by a "pressure" leak procedure [1]. An extensive series of structural analyses were then performed on these high-quality jammed packings. Prominent among other findings was the clear separation of the singular, $\delta(r)$, or contact contribution at $r=1$ (sphere diameter is taken as unit length $\sigma=1$ from now on) from the background, or near-contact contribution, the confirmation of the isostaticity of MRJ packings, and the splitting of the second peak in $g(r)$ as a clear signature of jamming.

In our recent simulations [40], the overall similarity between the pair-correlation function for monatomic hard spheres and for hard-sphere chains in the vicinity of the MRJ state was shown. It was established that for separations $r>1.1$, $g_{\text{chains}}(r)$ and $g_{\text{ss}}(r)$ for chains and for monomeric spheres are indistinguishable, within a small statistical uncertainty (<2.5%). Figure 3 shows the intermolecular pair radial distribution function $g_{\text{inter}}(r)$, the intramolecular pair density function $w_{\text{intra}}(r)$, and the total pair radial distribution $g_{\text{total}}(r)$, as obtained from present MC simulations on hard-sphere chains at the MRJ state, as functions of distance from contact $(r/\sigma)-1$, focusing in the vicinity of the split-second peak. Our simulation findings for $g_{\text{total}}(r)$ away from contact [reported in Fig. 3(c)] are in perfect qualitative and quantitative agreement with the simulation data from Donev *et al.* (Fig. 9 of [2]) and experimental ones by Aste *et al.* (Fig. 13 of [10]) for monomeric hard spheres. In particular, we were able to accurately identify the two characteristic peaks with the accompanying discontinuities at $r=\sqrt{3}\sigma$ and $r=2\sigma$, which is another strong indication of the simulated random chain assemblies that have reached their jammed state in a fashion analogous to monatomic hard-sphere packings. Furthermore, pairs of edge-sharing, coplanar, approximately equilateral triangles were found to account quite completely for the observed split-second peak in $g(r)$.

The inset of Fig. 4 shows the bending angle distribution $P(\theta)$, where $\theta=\cos^{-1}[(\vec{r}_{i+1}-\vec{r}_i)\cdot(\vec{r}_{i+2}-\vec{r}_{i+1})]$ and $\vec{r}$'s are position vectors of consecutive spheres. In an analogous fashion, the inset of Fig. 5 shows the torsion angle distribution $P(\phi)$, where

$$\phi=\cos^{-1}\times\frac{[(\vec{r}_{i+1}-\vec{r}_i)\times(\vec{r}_{i+2}-\vec{r}_{i+1})]\cdot[(\vec{r}_{i+3}-\vec{r}_{i+2})\times(\vec{r}_{i+2}-\vec{r}_{i+1})]}{|(\vec{r}_{i+1}-\vec{r}_i)\times(\vec{r}_{i+2}-\vec{r}_{i+1})|\cdot|(\vec{r}_{i+3}-\vec{r}_{i+2})\times(\vec{r}_{i+2}-\vec{r}_{i+1})|}.$$

Although the intensities of the maxima in $P(\theta)$ and $P(\phi)$ must be different from those in monomeric sphere MRJ packings, their positions are in perfect agreement as expected from the arguments presented in the Appendix. Their sharpness makes it also possible to unequivocally attribute them to specific geometric arrangements: the maxima at $\theta=60°$ and 120° in $P(\theta)$ correspond to two coplanar equilateral triangles sharing an edge and to three consecutive spheres on the vertices of one equilateral triangle, respectively. In the later case

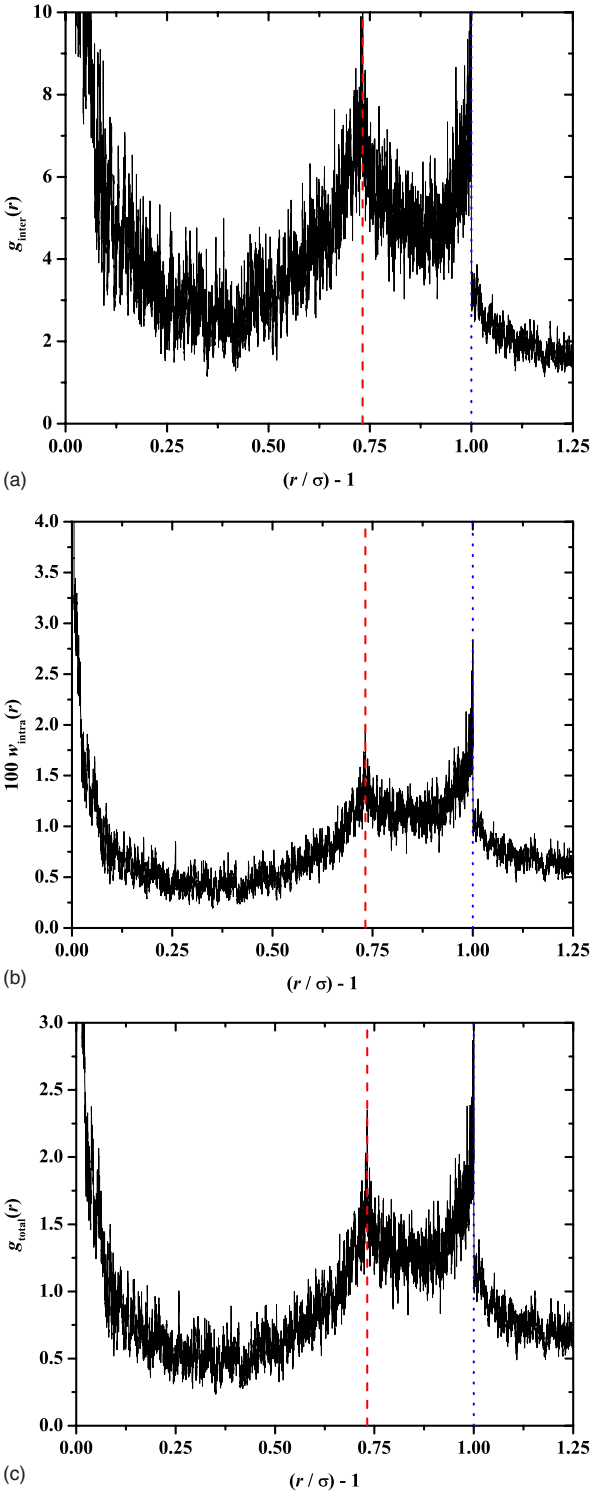

FIG. 3. (Color online) (a) Intermolecular pair radial distribution function $g_{\text{inter}}(r)$, (b) intramolecular pair density function $w_{\text{intra}}(r)$, and (c) total pair radial distribution function $g_{\text{total}}(r)$ as obtained from MC simulations on the $N=24$ hard-sphere chain system at the MRJ state. The plot is magnified so as to focus around the split-second peak. Also shown as guides for the eye are vertical lines to indicate the discontinuities at $r=\sqrt{3}\sigma$ and $r=2\sigma$. Noise in the distribution is due to the very narrow binning. In more standard plots, bin width is usually two orders of magnitude larger, resulting in very smooth $g(r)$, see for example [39,40,43,44] .

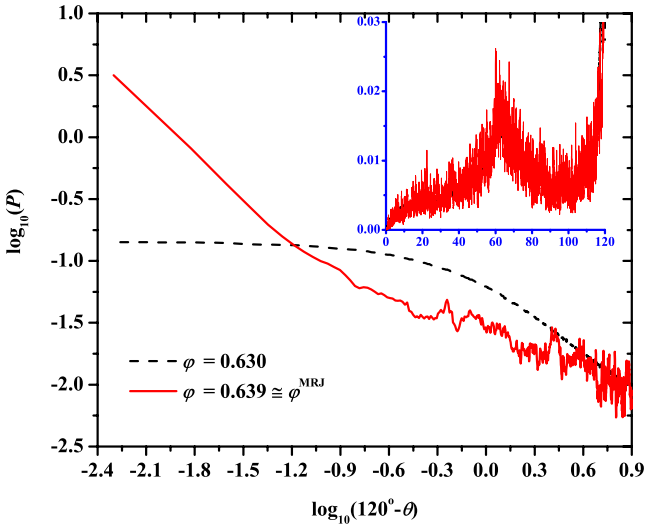

FIG. 4. (Color online) Inset: probability distribution for the supplement of bending angle θ from MC simulations for the $N=24$ system at volume fractions $\varphi=0.63$ and $\varphi=\varphi^{\mathrm{MRJ}}\simeq 0.639$. Bending angle is defined as the angle between two successive bonds along the chain. As in Fig. 3, noise in the distribution is due to the very narrow binning. Main: double-logarithmic plot of the probability distribution as a function of the divergence from the contact angle at $\theta_c=120°$ (since this value of the bending angle ensures contact for intramolecular neighbors that are separated by two bonds).

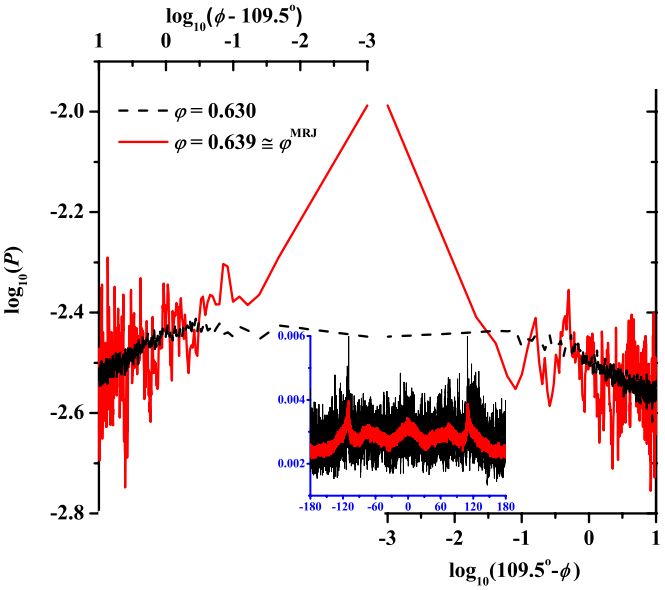

FIG. 5. (Color online) Inset: probability distribution for the torsion angle ϕ from MC simulations for the $N=24$ system at volume fractions $\varphi=0.63$ and $\varphi=\varphi^{\mathrm{MRJ}}\simeq 0.639$. Torsion angle is defined as the angle between the planes formed by successive triplets of spheres along the chain; all-trans conformation corresponds to 0°. As in Fig. 3, noise in the distribution is due to the very narrow binning. Main: double-logarithmic plot of the probability distribution as a function of the divergence from the characteristic torsion angle at $\phi_c=109.5°$ for (top/right axis): $\phi>\phi_c$ and (bottom/left axis): $\phi<\phi_c$.

($\theta=120°$) where the triplet forms the equilateral triangle spheres i and $i+2$ become perfectly tangent, each increases the number of contacts for the other sphere; consequently, the 1–3 arrangement of $\theta_c=120°$ can be considered as an effective contact angle. Similarly, $P(\phi)$ exhibits maxima centered around values of the torsion angle that correspond to four consecutive spheres occupying the vertices of vertex or edge sharing tetrahedral [44] leading to characteristic torsional conformations as denoted by the peaks at 0°, 54.7°, 70.5°, and 109.5°.

In the main panel of Fig. 4 we present in a double-logarithmic plot the probability distribution as a function of the divergence from the contact angle ($\theta_c=120°$) as obtained from present MC simulations at $\varphi=0.63$ and $\varphi=\varphi^{\mathrm{MRJ}}$. Particularly noteworthy is the sharp increase in the population of sites with bending conformations equal to the contact angle as we reach the vicinity of the MRJ state. The intensity in $P(\theta)$ at the MRJ state ($\varphi^{\mathrm{MRJ}}=0.639$) around $\theta_c=120°$ is found to be by a factor of approximately 30 higher than the corresponding one at $\varphi=0.63$. Similar conclusions can be drawn for the sharpness of the divergence at $\theta=60°$, which is directly comparable to that obtained in Ref. [2] for packings of monatomic hard spheres jammed to gaps on the order of $O(10^{-12})$. Identical trends are further observed for the 1–4 intramolecular packing arrangements as shown in the main panel of Fig. 5 for the torsion angle distribution $P(\phi)$. Here, the intensity at characteristic peak of $\phi_c=109.5°$ as we move from $\varphi=0.63$ to $\varphi=\varphi^{\mathrm{MRJ}}$ is increased by a factor of around 3. Albeit the fact that the difference in the intensities for the global maximum of the torsion angle is significantly smaller than the corresponding one ($\simeq 30$) for the bending contact angle, it is still appreciably evident. From the results depicted in Figs. 4 and 5, it is thus well established that significant changes occur in the bending and the torsional arrangements as the jammed state of random chain packings is approached.

The main objective of the present work is not to describe these arrangements in detail (which has been the focus of Ref. [44]), but to show that chain connectivity affords an unprecedented clear view of the contact network in MRJ assemblies of monatomic hard spheres. The reason is that the intramolecular contact between successive spheres along a chain makes a physically correct non-negligible contribution to all geometrical descriptors, thus yielding insights that could only be attained with the most precisely jammed packings of monomeric hard spheres (as, for example, those reported in Ref. [2]).

Jammed random packings of hard-sphere chains offer more obvious advantages in the detection of structural features involving higher number of spheres. A good example is the shared-neighbor analysis [2]. Thanks to the high quality of their strictly jammed packings, the modeling study of Ref. [2] represents the most precise investigation of the contact network of disordered hard-sphere assemblies to date. Unlike in the studies of Anikeenko and Medvedev [59], Donev *et al.* [2] could only identify very few tetrahedra in their shared-neighbor analysis. At a first sight this finding seems in partial contradiction with observations of extensive polytetrahedral structuring [59] in MRJ packings, although this discrepancy is due to the (intentional) loose definition of neighbors in

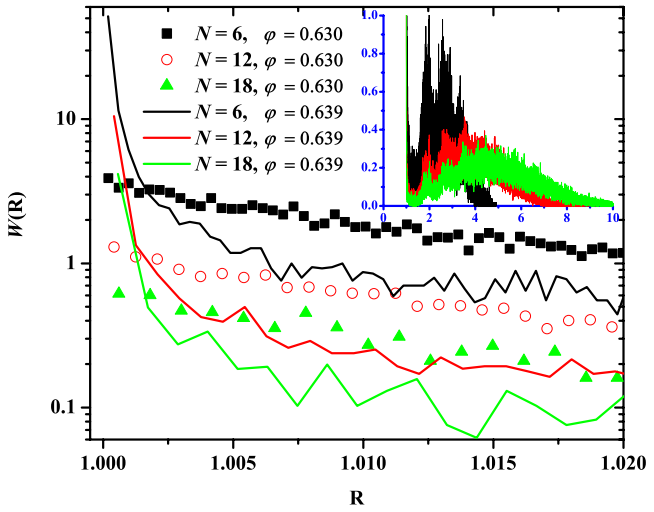

FIG. 6. (Color online) Inset: end-to-end vector distribution $W(\mathbf{R})$ for chains of lengths $N=6$, 12, and 18 at $\varphi=\varphi^{\mathrm{MRJ}}\simeq 0.639$. Main: linear-logarithmic scale of $W(\mathbf{R})$ versus $\mathbf{R}$ in the vicinity of the contact distance for chains of lengths $N=6$, 12, and 18 at $\varphi=0.63$ and at $\varphi=\varphi^{\mathrm{MRJ}}\simeq 0.639$.

Ref. [59]. Our present analysis of ensembles of chains in the close vicinity of the MRJ state tends to support the conclusions drawn in Ref. [2]. For example, the inset of Fig. 6 shows the orientation-averaged probability distribution of the end-to-end vector $4\pi r^2 W(\mathbf{r})$, for chains of lengths $N=6$, 12, and 18 at the MRJ state. The most prominent peaks in these distributions are centered around the values corresponding to consecutive spheres along the chain occupying sites on tetrahedra that share vertices, edges, or, much more rare, faces. Apart from confirming the scarcity of truly polytetrahedral aggregates [2], our analysis uncovers a remarkable feature: the distribution of the end-to-end vector displays a strong maximum at $r=1$, i.e., chains have an appreciable tendency to form *closed loops*. The main panel of Fig. 6 shows the probably divergent character of this contribution as the MRJ state is approached. The effect is of course more pronounced for short chains ($N=6$), but it is undeniably present for all chain lengths, as shown by the sharp increase in the probability of the end-to-end vector at $r=1$. The existence of contact rings at the MRJ is a consequence of "chain collapse," and of the prevalence of very compact chain conformations. In turn, the sharp decrease in chain dimensions, as quantified by several metrics of size at high volume fractions and especially in the marginal regime [41–44] is attributed to the adoption of specific bending and torsion angles corresponding to 1–3 and 1–4 intermolecular interactions, respectively. This tendency for the adoption of very compact conformations for the bonded geometry near the MRJ state can be further seen in the corresponding distributions of Figs. 4 and 5.

The structural characteristic of chain compactness and the formation of chain loops are vividly shown in Fig. 7 where arandomly selected configuration of the $N=12$ system at the MRJ state is shown with the coordinates of sphere centers subjected to periodic boundary conditions [Fig. 7(a)] and fully unwrapped in space [Fig. 7(b)]. In addition, in Figs. 7(c) and 7(d) only the chains that form rings are shown in atomistic detail [panel (c)] and with the backbones shown as

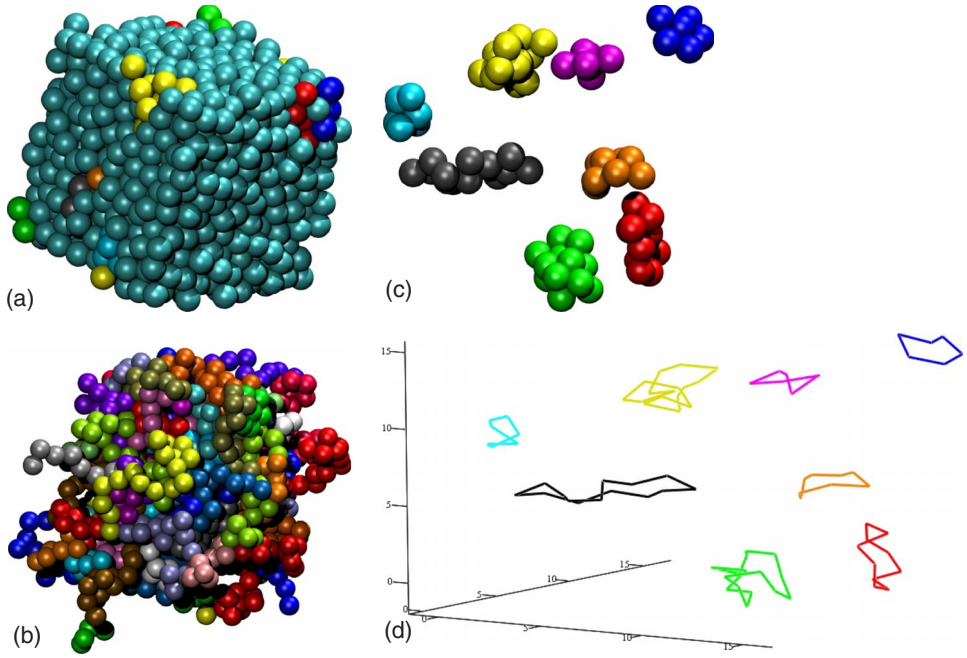

FIG. 7. (Color online) System configuration of a typical (randomly selected) frame from MC simulations on the $N=12$ system at the MRJ state. (a) coordinates of sphere centers are subjected to periodic boundary conditions (i.e., wrapped within the simulation cell) and sites of chains that form closed loops are colored differently, (b) coordinates of sphere centers are fully unwrapped in space and each site is colored according to its chain, and (c) only chains (unwrapped in space) that form closed loops are shown. In panel (d), the backbones of the same loop-forming chains are represented as a stereo pair. In this specific example 8 out of 100 polymers exhibit ringlike chain architecture ($\mathbf{R}=1$). Images (a)–(c) are created with the VMD software [60,61].

stereo pairs [panel (d)]. In this specific MC system configuration, 8% of the chains adopt conformations that correspond to loops ($r=1$).

Our present result seems to deviate from the analysis of Donev *et al.* [2] who found *open* clusters (in the form of chains) of up to five contacting particles to be the most prevalent geometrical pattern. We surmise that their lack of success in their search for closed loops may have been caused by the practical impossibility of carrying out a graph analysis to the required depth (in their studies tolerance for the detection of contact neighbors is up to machine accuracy). The strength of using the $\Xi^{\mathrm{MRJ}}_{\mathrm{chains}}$ ensemble for elucidating such "far-neighbor" structural issues is that (intramolecular) neighbors are trivially known by construction (as a direct consequence of chain connectivity), so that no search analysis is required and numerical precision is not a limitation. For example, in Ref. [59], typical tolerances for neighboring particles to be considered as forming a tetrahedron are up to nine orders of magnitude less stringent than in Ref. [2]. It is not surprising that the respective authors draw different conclusions. As pointed out in Ref. [2], this issue of numerical accuracy may become the limiting factor in the elucidation of structural aspects in hard-sphere systems. Although the $\Xi^{\mathrm{MRJ}}_{\mathrm{chains}}$ ensemble does not allow a quantitative prediction of peak intensities, it bypasses several vexing numerical problems in the detection of geometric patterns and qualitative features in MRJ structures.

Of particular importance for the prediction of mechanical properties of dense random packings is the average number of contacts or the mean coordination number $\langle Z\rangle$. Although its geometrical definition is unproblematic, the precise calculation of the mean coordination number is by no means trivial, especially for experimental samples [7,10]. This numerical ill-definition stems from the fact that a tolerance ("gap") has to be defined and used as the threshold below which a pair of spheres is considered to be contacting neighbors. It is widely accepted from numerous independent studies that jammed random packings of monomeric hard spheres fulfill the isostatic condition of having an average coordination number $\langle Z\rangle=2d$, where d is the dimensionality of the system [2,7,10]. In Fig. 8 we present the cumulative coordination number as a function of the contact gap between spheres as obtained from present MC simulations on the $N=24$ system at $\varphi=0.63$ and at the MRJ state. It is immediately apparent that for small gaps $(10^{-4},10^{-3})$ there is a significant difference in the qualitative and the quantitative behaviors of the two systems. For the dense one ($\varphi=0.63$) at very small gaps $\langle Z\rangle\approx 2$ resulting from the "inherent connectivity," as expected in chain systems due to the imposed connectivity, for all sites except chain ends which are inherently connected to a single sphere ($\langle Z\rangle=1$). The cumulative coordination continuously increases as the gap (tolerance) for intersphere distances is made less strict (i.e., detection of neighbors at further distances). In sharp contrast the mean coordination number at the MRJ state for tolerances about 10^{-4} is slightly smaller than 4 (a value which is twice as high as the expected inherent coordination) with a trend to rapidly increase. At gaps on the order of 10^{-3} (which is the order magnitude of the accuracy of the present MC simulations), the cumulative $\langle Z\rangle$ reaches a plateau value of 6 (for a relatively small range of gaps from contact), as expected by the isostaticity condition and as observed in simulations and experiments of jammed random packings of single-sphere analogs [2,7,10]. The significant qualitative differences in the coordination number and accordingly in the fulfillment of the isostaticity condition between dense ($\varphi=0.63$) and jammed ($\varphi=\varphi^{\mathrm{MRJ}}$) chain configurations are evident from the connectivity graphs in Fig. 9. There, we present system configurations in a ball&stick representation (in which sphere radii have been appropriately reduced for clarity) by taking into account the inherent coordination as imposed by chain connectivity and by detecting the contacting neighbors based solely on proximity criteria independent of chain connectivity. For the latter the threshold value for the detection of a bond is taken equal to the gap required for $\langle Z\rangle$ to reach the expected plateau value of 6 at the MRJ state as shown in Fig. 8. It is immediately apparent that while the inherent coordination is obviously independent of the volume fraction and the same in both cases, the connectivity network as quantified by the cumulative coordination is far richer at the MRJ ($\varphi=0.639$) state than at $\varphi=0.63$.

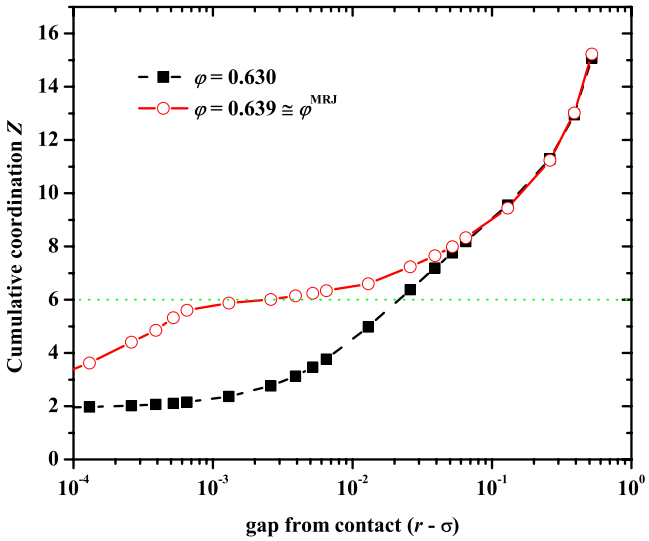

FIG. 8. (Color online) Cumulative coordination number Z as a function of the gap between spheres $(r-\sigma)$ in logarithmic-linear scale from MC simulations on the $N=24$ system at volume fractions $\varphi=0.63$ and $\varphi=\varphi^{\mathrm{MRJ}}\simeq 0.639$. Also shown by the horizontal dotted line is the theoretical expectation of $Z=2d$ from the isostatic condition where d is the dimensionality of the system.

We should particularly note that in the work of Donev *et al.* [2] the computations are so accurate that they are able to recover the plateau of 6, and thus verify the isostaticity of the jammed packings of monomeric hard spheres for gaps as low as $O(10^{-12})$. Our present results fall short of such a high numerical precision due to obvious computational demands related to the modeling of macromolecular counterparts. Simulations are currently in progress in order to generate jammed random packings of hard-sphere chains to full numerical precision.

IV. CONCLUSIONS

We have presented results about the salient structural features of jammed random packings of linear freely jointed

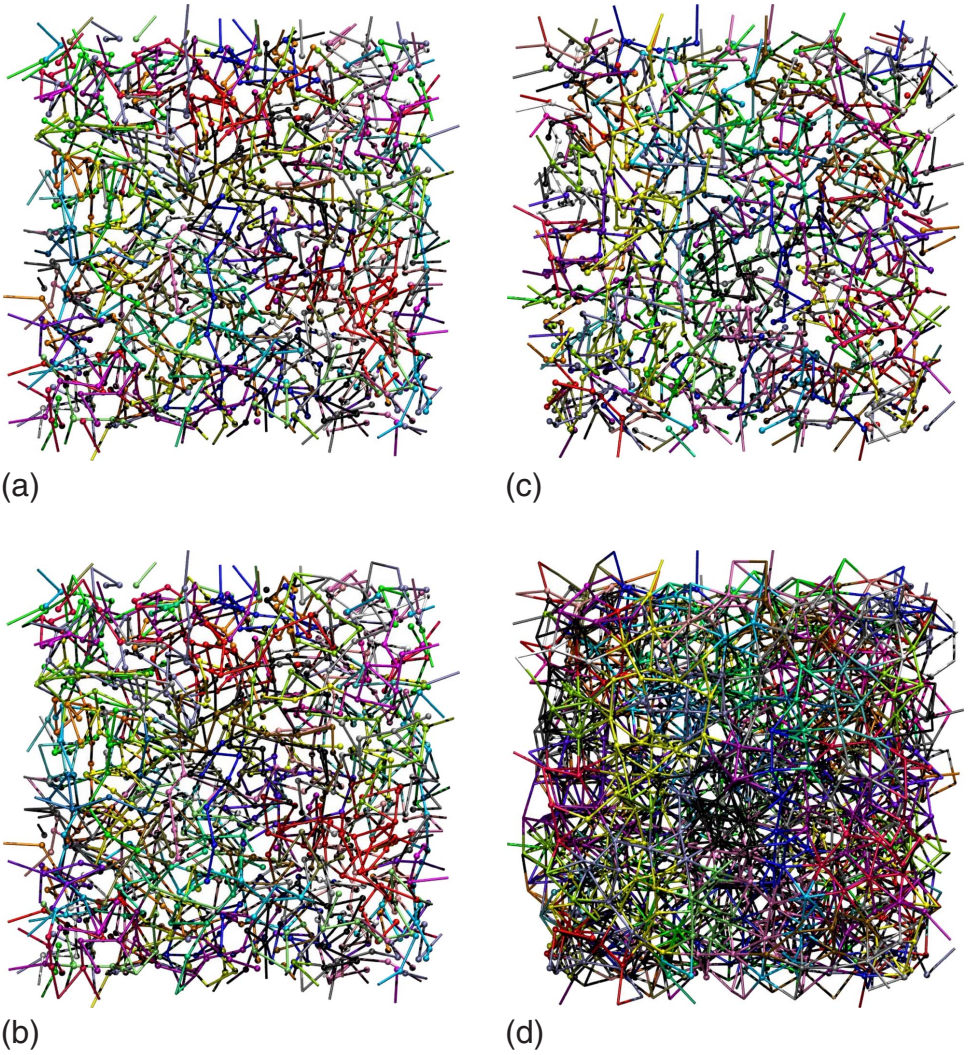

FIG. 9. (Color online) System configurations at [left: (a) and (b)]: $\varphi=0.63$ and [right: (c) and (d)]: $\varphi=\varphi^{\mathrm{MRJ}}=0.639$. The ball&stick representation is adopted with reduced sphere radius for visual purposes. Sites are colored according to the identity of their parent chain (online version). Bonds are constructed according to [top: (a) and (c)] the "inherent coordination" as imposed by the double tangency condition as a result of chain connectivity and [bottom: (b) and (d)] the proximity condition independent for a pair being in the same or different chains. In the latter case (right panels) the threshold value for the identification of a bond is the value for which the plateau of $Z=6$ is obtained for the cumulative coordination at the MRJ state (see also Fig. 8). A bond that is affected by periodic boundary conditions appears as a dangling bond emanating from one site of the bonded pair. Image is created with the VMD software [60,61].

chains of tangent hard spheres as obtained from very long MC simulations. We have shown that the chain configurations at the highest simulated volume fraction remain disordered and jammed by continuously tracking the evolution of the CCE norms and the portion of flippers, respectively. The pair radial distribution function near the split-second peak is in striking agreement with the corresponding one obtained for monatomic analogs at the MRJ state. We further detect a large number of linear chains that adopt conformations that correspond to closed loops, a trend that increases significantly as we approach the MRJ state. Our generated and relaxed chain packings at the MRJ state unavoidably lack the numerical accuracy or detail achieved in recent state-of-the-art modeling studies of monatomic analogs by Donev *et al.* [2] However, we are still able to detect significant differences in the contact network between dense and jammed disordered chain packings and to confirm that the isostaticity condition for the contact network at the MRJ state is fulfilled. Based on the above findings, we propose an exact correspondence between the ensembles of monatomic hard spheres and of hard-sphere chains that offers insights for the structural characteristics of the MRJ state. We have shown that random assemblies of monomeric hard spheres and of chains of tangent hard spheres share several key structural characteristics at the MRJ state. It is thus established that the structural behavior at the MRJ state in many key aspects is general and universal, being affected neither by the holonomic constraints imposed by chain connectivity nor by the simulation protocol employed for the generation of the samples.

ACKNOWLEDGMENTS

This work was supported by the EC through Contract No. NMP3-CT-2005-016375 and by the CICYT through Contract No. MAT2005-25569-E. Allocation of computational time on the "magerit" supercomputer of CeSViMa (UPM, Spain) and on CSCS (Switzerland) is gratefully acknowledged.

APPENDIX

The goal of this appendix is to make precise the relationship that exists at the MRJ state between the ensemble of configurations of the hard-sphere chain system $\Xi_{\mathrm{chains}}^{\mathrm{MRJ}}$ and the ensemble $\Xi_{\mathrm{ss}}^{\mathrm{MRJ}}$ of configurations of the monatomic hard-sphere system. A key feature of the statistical mechanics of jammed systems is that, although a great deal of numerical evidence is available for some of the most basic results (e.g., the value of the volume fraction occupied by the spheres at

the MRJ, the pair radial distribution function), no analytical derivation has yet been found for them. In the following we will proceed pragmatically by accepting a numerically proven observation as a highly plausible postulate in which to build the correspondence between configurations of monomeric spheres and of chains of spheres.

Let a given configuration of the system composed of N_{sites} identical hard spheres at the MRJ state in a fixed volume V be labeled by the index j (see Fig. 2). As both N_{sites}, $V \to \infty$, $\varphi \to \varphi_{\text{ss}}^{\text{MRJ}}$. This jth configuration is fully described by the list $\mathbf{R}_j$ (of length $3N_{\text{sites}}$) of the position vectors of the centers $\mathbf{r}^{(i)}$ of its N_{sites} spheres, i.e., $\mathbf{R}_j \equiv \{\cup_{i=1}^{N_{\text{sites}}} \mathbf{r}^{(i)}\}$. Then, $\Xi_{\text{ss}}^{\text{MRJ}} \equiv \{\mathbf{R}_j\}$ is the complete set, or ensemble, of configurations of the N_{sites} hard spheres at the MRJ state. Transformations of $\mathbf{R}_j$ by the (continuous) translation, proper and improper orthogonal, and (discrete) subindex permutation groups are excluded from $\Xi_{\text{ss}}^{\text{MRJ}}$. Each $\mathbf{R}_j$ in $\Xi_{\text{ss}}^{\text{MRJ}}$ is then a physically unique member of this ensemble. Analogously, each element of the ensemble $\Xi_{\text{chains}}^{\text{MRJ}}$ is fully characterized by the set of position vectors $\mathbf{R}_j$ of the N_{sites} spheres that build the chains and a matrix [62] $\mathbf{C}_k$ (of size $N_{\text{sites}} \times N_{\text{sites}}$) of sphere labels that defines the connectivity among the spheres: $\Xi_{\text{chains}}^{\text{MRJ}} \equiv \{(\mathbf{R}_j, \mathbf{C}_k)\}$. Let us also accept the following postulate, the validity of which will be discussed below:

Postulate. For every configuration $\mathbf{R}_j \in \Xi_{\text{ss}}^{\text{MRJ}}$, it is possible to generate a number $n(\mathbf{R}_j)$ of configurations $(\mathbf{R}_j, \mathbf{C}_k) \in \Xi_{\text{chains}}^{\text{MRJ}}$ that share $\mathbf{R}_j$ and differ only in $\mathbf{C}_k$, and this number $n(\mathbf{R}_j)$ of configurations is of the same order $O(\cdots)$ (in Bachmann-Landau notation [63]) for all configurations $\mathbf{R}_j \in \Xi_{\text{ss}}^{\text{MRJ}}$.

Regarding the validity of the Postulate, although no general analytical proof exists for it, algorithms that able to link the individual spheres of an MRJ configuration $\mathbf{R}_j \in \Xi_{\text{ss}}^{\text{MRJ}}$ into chains of predetermined length are known and have been shown to work in all specific cases [56]. Furthermore, for a system composed of N_{sites} hard spheres at the MRJ, the number $n(\mathbf{R}_j)$ of connectivity matrices, i.e., the number of possible ways of connecting the N_{sites} spheres so as to form N_{chains} chains of length N, such that $N_{\text{chains}}N = N_{\text{sites}}$, is given by the following mean-field estimate [64]:

$$n(\mathbf{R}_j) = N^{N_{\text{chains}}} \left(\frac{\langle Z \rangle - 1}{N_{\text{sites}}} \right)^{N_{\text{chains}}(\langle Z \rangle - 1)}. \tag{A1}$$

In practice, for a given $\mathbf{R}_j \in \Xi_{\text{ss}}^{\text{MRJ}}$, algorithms in combinatorial geometry algorithms are able to generate a number of connectivities, which scale at least exponentially with the number of spheres: $n(\mathbf{R}_j) \geq O[\exp(N_{\text{sites}})]$. There is thus, in addition, overwhelming numerical evidence of the correctness of the Postulate. It is in fact a very weak assumption, and, as a consequence, it is very often assumed to be "self-evident" by physicists [64].

The first implication of the postulate is that the volume fraction φ occupied by the hard spheres at the MRJ state is the same both for monatomic (single) hard spheres and for linear chains of hard spheres $\varphi_{\text{chains}}^{\text{MRJ}} = \varphi_{\text{ss}}^{\text{MRJ}}$. The Postulate guarantees the condition $\varphi_{\text{chains}}^{\text{MRJ}} \geq \varphi_{\text{ss}}^{\text{MRJ}}$. It is however trivial to show that $\varphi_{\text{chains}}^{\text{MRJ}} \leq \varphi_{\text{ss}}^{\text{MRJ}}$ must also hold: if we assume $\varphi_{\text{chains}}^{\text{MRJ}} > \varphi_{\text{ss}}^{\text{MRJ}}$ (strict inequality), there would exist an ensemble in which hard-sphere chains would pack strictly more densely than single spheres. One could then remove the bonds in all chains in each configuration of this ensemble [65]. The result would be an ensemble of hard spheres of the same density as the starting chain system, in contradiction with the hypothesis. Thus, $\varphi_{\text{chains}}^{\text{MRJ}} = \varphi_{\text{ss}}^{\text{MRJ}}$ must hold. Recent numerical evidence [40] for $\varphi_{\text{chains}}^{\text{MRJ}} = \varphi_{\text{ss}}^{\text{MRJ}}$ is in agreement with this equality, which further strengthens the plausibility of the Postulate.

The point we want to address in this appendix is a straightforward one that involves the cardinality (in loose terms, the size) of the ensembles. In the thermodynamic limit, the ensemble of single-sphere (monomeric) configurations $\Xi_{\text{ss}}^{\text{MRJ}}$ is an infinite set which has the cardinality of the continuum $\aleph_1$. As a consequence of the Postulate, we can associate with each $\mathbf{R}_j \in \Xi_{\text{ss}}^{\text{MRJ}}$ a number of configurations $(\mathbf{R}_j, \mathbf{C}_k) \in \Xi_{\text{chains}}^{\text{MRJ}}$. In the thermodynamic limit N_{sites}, $V \to \infty$, this set of chain configurations associated with one specific $\mathbf{R}_j \in \Xi_{\text{ss}}^{\text{MRJ}}$ is also of infinite size, given by $\lim_{N_{\text{sites}} \to \infty} n(\mathbf{R}_j)$, but it is a countably infinite set, i.e., its cardinality is $\aleph_0$ and not $\aleph_1$ as it would be for the power set (the set of all possible subsets) of the N_{sites} spheres. This is a consequence of the appearance of N_{sites} in Eq. (A1) and ultimately of the existence of connectivity. Hence, the ensemble of chain configurations $\Xi_{\text{chains}}^{\text{MRJ}}$ has the cardinality of the Cartesian product of two infinite sets, one of cardinality $\aleph_1$ and one of $\aleph_0$, which is again $\aleph_1$ (in compact notation $\aleph_1 \aleph_0 = \aleph_1$) [66]. Furthermore, the randomness of the MRJ state, i.e., the absence of distinguished configurations in $\Xi_{\text{ss}}^{\text{MRJ}}$, guarantees that the scaling of $n(\mathbf{R}_j)$ with N_{sites} [Eq. (A1)] must be the same for all $\mathbf{R}_j \in \Xi_{\text{ss}}^{\text{MRJ}}$.

Thus, the relationship that exists at the MRJ state between the ensemble of configurations of the hard-sphere chain system $\Xi_{\text{chains}}^{\text{MRJ}}$ and the ensemble $\Xi_{\text{ss}}^{\text{MRJ}}$ of configurations of the monatomic hard-sphere system is a many-to-one (surjective) correspondence between the members of these two ensembles. Every member of $\Xi_{\text{chains}}^{\text{MRJ}}$ is mapped onto a unique element of $\Xi_{\text{ss}}^{\text{MRJ}}$ by the surjective correspondence $F_{\text{chains}\to\text{ss}}: \Xi_{\text{chains}}^{\text{MRJ}} \to \Xi_{\text{ss}}^{\text{MRJ}}$, $(\mathbf{R}_j, \mathbf{C}_k) \mapsto \mathbf{R}_j$. As a consequence, $\Xi_{\text{chains}}^{\text{MRJ}}$ splits in equivalence classes by the action of $F_{\text{chains}\to\text{ss}}$, and every $\mathbf{R}_j$ is a class representative of the smaller ensemble $\Xi_{\text{ss}}^{\text{MRJ}} = \Xi_{\text{chains}}^{\text{MRJ}} / F_{\text{chains}\to\text{ss}}$ formed from $\Xi_{\text{chains}}^{\text{MRJ}}$ by the action of $F_{\text{chains}\to\text{ss}}$. Members (chains) of the $\mathbf{R}_j$ equivalence class of $\Xi_{\text{chains}}^{\text{MRJ}}$ are obtained by connecting the spheres in the configuration $\mathbf{R}_j \in \Xi_{\text{ss}}^{\text{MRJ}}$ in all possible ways (all possible connectivities $\mathbf{C}_k$) compatible with the prescribed chain length distribution.

We now consider the classical partition functions Z (not to be confused with the average coordination number $\langle Z \rangle$) of the ensembles $\Xi_{\text{ss}}^{\text{MRJ}}$ and $\Xi_{\text{chains}}^{\text{MRJ}}$. Formally,

$$Z_{\text{ss}}^{\text{MRJ}} = \sum_{i=1}^{|\Xi_{\text{ss}}^{\text{MRJ}}|} 1 = |\Xi_{\text{ss}}^{\text{MRJ}}| = \int_{\Omega} dR^{3N_{\text{sites}}}, \tag{A2}$$

where $|\Xi_{\text{ss}}^{\text{MRJ}}|$ is the size of $\Xi_{\text{ss}}^{\text{MRJ}}$ and the entire difficulty of computing $Z_{\text{ss}}^{\text{MRJ}}$ lies in determining the region of integration Ω in the $3N_{\text{sites}}$-dimensional configurational space in which

Ξ_{ss}^{MRJ} is defined. The probability distribution function of configurations in this ensemble is uniform and trivially given by

$$f_{ss}^{MRJ}(\mathbf{R}_j) = \frac{1}{Z_{ss}^{MRJ}}, \quad \forall\, \mathbf{R}_j. \tag{A3}$$

In practice, individual configurations are often generated with their proper probability (A3) by molecular dynamics (MD) methods [2,3].

The partition function of the ensemble Ξ_{chains}^{MRJ} is formally identical,

$$Z_{chains}^{MRJ} = \sum_{i=1}^{|\Xi_{chains}^{MRJ}|} 1 = |\Xi_{chains}^{MRJ}| = \int_{\Omega} dR^{3N_{sites}} n(\mathbf{R}), \tag{A4}$$

where now an additional difficulty appears in the determination of $n(\mathbf{R})$. The probability distribution function of configurations in this ensemble is given by

$$f_{chains}^{MRJ}(\mathbf{R}_j, \mathbf{C}_k) = \frac{1}{Z_{chains}^{MRJ}}, \quad \forall\, \mathbf{R}_j, \mathbf{C}_k. \tag{A5}$$

In practice, generating individual configurations of Ξ_{chains}^{MRJ} with their proper probability requires the use of advanced Monte Carlo (MC) methods [39,40].

The Postulate guarantees that the partition function (A4) can be factorized as

$$Z_{chains}^{MRJ} = \sum_{i=1}^{|\Xi_{ss}^{MRJ}|} \sum_{k=1}^{n(\mathbf{R}_i)} 1 = \sum_{i=1}^{|\Xi_{ss}^{MRJ}|} n(\mathbf{R}_i), \tag{A6}$$

where $n(\mathbf{R}_i)$ is the number of configurations $(\mathbf{R}_i, \mathbf{C}_k) \in \Xi_{chains}^{MRJ}$ that share $\mathbf{R}_i$ and differ only in connectivity $\mathbf{C}_k$ (in other words, the size of the equivalence class represented by $\mathbf{R}_i$). We can now write the probability with which a given $\mathbf{R}_i$ appears in the ensemble Ξ_{chains}^{MRJ}, irrespective of connectivity, i.e., its marginal or contracted distribution with respect to $\mathbf{C}_k$, $fc_{chains}^{MRJ}(\mathbf{R}_j)$,

$$fc_{chains}^{MRJ}(\mathbf{R}_i) = \frac{\sum_{k=1}^{n(\mathbf{R}_i)} 1}{Z_{chains}^{MRJ}} = \frac{n(\mathbf{R}_i)}{Z_{chains}^{MRJ}}. \tag{A7}$$

Thus, whereas in $f_{ss}^{MRJ}(\mathbf{R}_j)$ all single-sphere configurations $\mathbf{R}_j$ appear with equal probability, the same single-sphere configuration $\mathbf{R}_j$ appears in $fc_{chains}^{MRJ}(\mathbf{R}_j)$ with a probability proportional to the number of ways the monatomic spheres in $\mathbf{R}_j$ can be connected to form a configuration of chains. Thus, the configurations $\mathbf{R}_j$, which are equiprobable in Ξ_{ss}^{MRJ}, will have different weights in Ξ_{chains}^{MRJ} and will contribute proportionally to the ensemble average of any given observable A as follows

$$\langle A \rangle_{chains}^{MRJ} = \frac{n(\mathbf{R}_i) A(\mathbf{R}_i)}{Z_{chains}^{MRJ}} = fc_{chains}^{MRJ}(\mathbf{R}_i) A(\mathbf{R}_i), \tag{A8}$$

whereas in the ensemble of single (monomeric) spheres

$$\langle A \rangle_{ss}^{MRJ} = \frac{A(\mathbf{R}_i)}{Z_{ss}^{MRJ}}. \tag{A9}$$

Ensemble-average properties will be different for monatomic spheres and for chains because of the different statistical-mechanical weights of $\mathbf{R}_i$ in both ensembles: while a given single-sphere configuration $\mathbf{R}_i$ contributes a (relative) weight of 1 to the partition function of Ξ_{ss}^{MRJ}, its contribution to Ξ_{chains}^{MRJ} is proportional to the number of ways the spheres in configuration $\mathbf{R}_i$ can be joined obeying a predetermined connectivity. Although in general not very large, such differences in macroscopic averages must exist and have in fact been found in the radial pair distribution function, pressure, etc. [40]. The key point of this appendix is that the $\aleph_0$ cardinality of the equivalence classes $\mathbf{R}_i$ ensures that the weights $fc_{chains}^{MRJ}(\mathbf{R}_i)$ are neither divergent nor zero for all $\mathbf{R}_i$. This conclusion would not be warranted if the equivalence classes $\mathbf{R}_i$ were uncountably infinite in the thermodynamic limit, i.e., if they had cardinality $\aleph_1$.

Therefore, if a macroscopic observable is found to have a nonvanishing value in Ξ_{chains}^{MRJ}, it must necessarily have a (possibly different) but nonvanishing value in the single-sphere MRJ ensemble Ξ_{ss}^{MRJ}. The argument is valid not only for macroscopic observables, but it applies to structural features as well: if a given structural feature exists in Ξ_{chains}^{MRJ}, it must necessarily exist in Ξ_{ss}^{MRJ} as well with a possibly different but nonvanishing probability. Thus, packings of tangent hard-sphere chains at the MRJ state can yield valuable geometrical insights into the structure of MRJ assemblies of monatomic hard spheres.

[1] S. Torquato, T. M. Truskett, and P. G. Debenedetti, Phys. Rev. Lett. **84**, 2064 (2000).
[2] A. Donev, S. Torquato, and F. H. Stillinger, Phys. Rev. E **71**, 011105 (2005).
[3] A. Donev, F. H. Stillinger, and S. Torquato, Phys. Rev. Lett. **96**, 225502 (2006).
[4] F. Zamponi, Philos. Mag. **87**, 485 (2007).
[5] F. Zamponi, Nature (London) **453**, 606 (2008).
[6] W. P. Krekelberg, J. Mittal, V. Ganesan, and T. M. Truskett, Phys. Rev. E **77**, 041201 (2008).
[7] J. Brujic, C. M. Song, P. Wang, C. Briscoe, G. Marty, and H. A. Makse, Phys. Rev. Lett. **98**, 248001 (2007).
[8] C. Briscoe, C. Song, P. Wang, and H. A. Makse, Phys. Rev. Lett. **101**, 188001 (2008).
[9] C. Song, P. Wang, and H. A. Makse, Nature (London) **453**, 629 (2008).
[10] T. Aste, M. Saadatfar, and T. J. Senden, Phys. Rev. E **71**, 061302 (2005).
[11] A. V. Anikeenko, N. N. Medvedev, and T. Aste, Phys. Rev. E **77**, 031101 (2008).
[12] T. Aste and T. Di Matteo, Eur. Phys. J. B **64**, 511 (2008).
[13] C. S. O'Hern, S. A. Langer, A. J. Liu, and S. R. Nagel, Phys. Rev. Lett. **88**, 075507 (2002); C. S. O'Hern, L. E. Silbert, A. J. Liu, and S. R. Nagel, Phys. Rev. E **68**, 011306 (2003).
[14] N. Xu, J. Blawzdziewicz, and C. S. O'Hern, Phys. Rev. E **71**, 061306 (2005).

[15] L. Bowen, R. Lyons, C. Radin, and P. Winkler, Phys. Rev. Lett. **96**, 025701 (2006).
[16] J. D. Bernal, Nature (London) **185**, 68 (1960).
[17] G. D. Scott, K. R. Knight, and J. D. Bernal, Nature (London) **194**, 956 (1962).
[18] J. D. Bernal and J. L. Finney, Discuss. Faraday Soc. **43**, 62 (1967).
[19] A. Duri, D. A. Sessoms, V. Trappe, and L. Cipelletti, Phys. Rev. Lett. **102**, 085702 (2009).
[20] A. S. Keys, A. R. Abate, S. C. Glotzer, and D. J. Durian, Nat. Phys. **3**, 260 (2007).
[21] S. Slotterback, M. Toiya, L. Goff, J. F. Douglas, and W. Losert, Phys. Rev. Lett. **101**, 258001 (2008).
[22] C. Radin, J. Stat. Phys. **131**, 567 (2008).
[23] Z. Gaygadzhiev, M. Corredig, and M. Alexander, Langmuir **24**, 3794 (2008).
[24] M. Doi and S. F. Edwards, *The Theory of Polymer Dynamics* (Clarendon, Oxford, 1986).
[25] W. S. Jodrey and E. M. Tory, Phys. Rev. A **32**, 2347 (1985).
[26] J. Tobochnik and P. M. Chapin, J. Chem. Phys. **88**, 5824 (1988).
[27] B. D. Lubachevsky and F. H. Stillinger, J. Stat. Phys. **60**, 561 (1990).
[28] P. V. Krishna Pant and D. N. Theodorou, Macromolecules **28**, 7224 (1995); N. C. Karayiannis, V. G. Mavrantzas, and D. N. Theodorou, Phys. Rev. Lett. **88**, 105503 (2002); N. C. Karayiannis, A. E. Giannousaki, V. G. Mavrantzas, and D. N. Theodorou, J. Chem. Phys. **117**, 5465 (2002); K. Foteinopoulou, N. C. Karayiannis, M. Laso, and M. Kröger, J. Phys. Chem. B **113**, 442 (2009).
[29] A. Yethiraj and C. K. Hall, J. Chem. Phys. **96**, 797 (1992).
[30] A. Yethiraj and R. Dickman, J. Chem. Phys. **97**, 4468 (1992).
[31] R. Chang and A. Yethiraj, Phys. Rev. Lett. **96**, 107802 (2006).
[32] K. Koniaris and M. Muthukumar, Phys. Rev. Lett. **66**, 2211 (1991).
[33] A. P. Malanoski and P. A. Monson, J. Chem. Phys. **107**, 6899 (1997).
[34] F. A. Escobedo and J. J. de Pablo, J. Chem. Phys. **102**, 2636 (1995).
[35] F. A. Escobedo and J. J. de Pablo, J. Chem. Phys. **106**, 9858 (1997).
[36] A. J. Haslam, G. Jackson, and T. C. B. McLeish, Macromolecules **32**, 7289 (1999).
[37] M. Kröger, Comput. Phys. Commun. **118**, 278 (1999).
[38] M. Kröger, M. Müller, and J. Nievergelt, CMES–Comput. Model. Eng. Sci. **4**, 559 (2003).
[39] N. C. Karayiannis and M. Laso, Macromolecules **41**, 1537 (2008).
[40] N. C. Karayiannis and M. Laso, Phys. Rev. Lett. **100**, 050602 (2008).
[41] M. Laso and N. C. Karayiannis, J. Chem. Phys. **128**, 174901 (2008).
[42] K. Foteinopoulou, N. C. Karayiannis, M. Laso, M. Kröger, and M. L. Mansfield, Phys. Rev. Lett. **101**, 265702 (2008).
[43] M. Laso, N. C. Karayiannis, K. Foteinopoulou, M. L. Mansfield, and M. Kröger, Soft Matter **5**, 1762 (2009).
[44] N. C. Karayiannis, K. Foteinopoulou, and M. Laso, J. Chem. Phys. **130**, 164908 (2009).
[45] N. C. Karayiannis, K. Foteinopoulou, and M. Laso, J. Chem. Phys. **130**, 074704 (2009).
[46] N. C. Karayiannis, K. Foteinopoulou, and M. Laso, Phys. Rev. Lett. (in press).
[47] M. A. Denlinger and C. K. Hall, Mol. Phys. **71**, 541 (1990).
[48] N. Sushko, P. van der Schoot, and M. A. J. Michels, J. Chem. Phys. **115**, 7744 (2001).
[49] We use the term flipper (as opposed to "jammed") in a general sense to denote a site that is able to perform a minimal displacement in the form of a flip move (for all spheres that lie in the internal of the chain, i.e., spheres with two bonds) or of a rotation move (for spheres that constitute chain ends, i.e., spheres with one bond). We use the number of remaining flippers to quantify the proximity to the MRJ state for chains, just as the number of "rattlers" is used to quantify jamming in random packings of monomeric hard spheres (see Ref. [1] for more details).
[50] M. D. Rintoul and S. Torquato, Phys. Rev. Lett. **77**, 4198 (1996).
[51] www.qhull.org
[52] As shown in Ref. [45] the CCE norm by construction is highly discriminating in the detection of local order: a site of HCP-like character cannot simultaneously have a low FCC-CCE norm and vice versa.
[53] T. Aste, M. Saadatfar, A. Sakellariou, and T. J. Senden, Physica A **339**, 16 (2004).
[54] P. J. Steinhardt, D. R. Nelson, and M. Ronchetti, Phys. Rev. B **28**, 784 (1983).
[55] The common signature of local conformations reported in the original work in Ref. [53] is further verified by our structural analysis based on the rotationally invariant measures on dense chain packings [44,45]. This limited ability to discriminate between competing crystal types was the motivation behind the introduction of the CCE norms.
[56] J. Pach and P. K. Agarwal, *Combinatorial Geometry* (John Wiley, New York, 1995).
[57] A. Donev, S. Torquato, and F. H. Stillinger, J. Comput. Phys. **202**, 737 (2005); A. Donev, S. Torquato, and F. H. Stillinger, *ibid.* **202**, 765 (2005).
[58] B. D. Lubachevsky, F. H. Stillinger, and E. N. Pinson, J. Stat. Phys. **64**, 501 (1991).
[59] A. V. Anikeenko and N. N. Medvedev, Phys. Rev. Lett. **98**, 235504 (2007).
[60] W. Humphrey, A. Dalke, and K. Schulten, J. Mol. Graphics **14**, 33 (1996).
[61] VMD, Molecular Modeling and Visualization Program, Version 1.8.6, Theoretical and Computational Biophysics Group, University of Illinois and Beckman Institute, http://www.ks.uiuc.edu/Research/vmd
[62] The $N_{\text{sites}} \times N_{\text{sites}}$ matrix $\mathbf{C}_k$ is required for a general chain system of arbitrary connectivity, i.e., linear, multibranched, "pompon," star shaped, dendrimeric, cross linked, etc. In most practical cases, $\mathbf{C}_k$ is sparse. For linear chains, a more economical tridiagonal $\mathbf{C}_k$ would suffice.
[63] N. G. de Bruijn, *Asymptotic Methods in Analysis* (Dover Publications, New York, 1981).
[64] This estimate can be obtained by removing the assumption of diluted solution in the Flory-Huggins formalism.
[65] Z. H. Stachurski, Phys. Rev. Lett. **90**, 155502 (2003).
[66] N. Biggs, *Discrete Mathematics* (Oxford University Press, Oxford, 2002).